Hindawi Publishing Corporation
Journal of Ceramics
Volume 2014, Article ID 874034, 10 pages
http://dx.doi.org/10.1155/2014/874034

Research Article

Durability Modeling of Environmental Barrier Coating (EBC) Using Finite Element Based Progressive Failure Analysis

Ali Abdul-Aziz,[1] Frank Abdi,[2] Ramakrishna T. Bhatt,[1] and Joseph E. Grady[1]

[1] *NASA Glenn Research Center, Cleveland, OH 44135, USA*
[2] *AlphaSTAR Corporation, Long Beach, CA 90804, USA*

Correspondence should be addressed to Ali Abdul-Aziz; ali.abdul-aziz-1@nasa.gov

Received 28 October 2013; Accepted 14 January 2014; Published 9 April 2014

Academic Editor: Guillaume Bernard-Granger

The necessity for a protecting guard for the popular ceramic matrix composites (CMCs) is getting a lot of attention from engine manufacturers and aerospace companies. The CMC has a weight advantage over standard metallic materials and more performance benefits. However, these materials undergo degradation that typically includes coating interface oxidation as opposed to moisture induced matrix which is generally seen at a higher temperature. Additionally, other factors such as residual stresses, coating process related flaws, and casting conditions may influence the degradation of their mechanical properties. These durability considerations are being addressed by introducing highly specialized form of environmental barrier coating (EBC) that is being developed and explored in particular for high temperature applications greater than 1100°C. As a result, a novel computational simulation approach is presented to predict life for EBC/CMC specimen using the finite element method augmented with progressive failure analysis (PFA) that included durability, damage tracking, and material degradation model. The life assessment is carried out using both micromechanics and macromechanics properties. The macromechanics properties yielded a more conservative life for the CMC specimen as compared to that obtained from the micromechanics with fiber and matrix properties as input.

1. Introduction

Durability and damage related issues concerning fiber reinforced ceramic matrix composites (FRCMC), specifically SiC fiber reinforced SiC matrix composites (SiC/SiC), are of significance for low maintenance, dependability, and cost efficiency. Typically, most of damage and failure are caused by environmental conditions. These conditions are confined to moisture, thermal-mechanical load, creep, and fatigue. Lab, burner rig, and field tests have been performed to capture the service environment, induced damage, and resulting strength/stiffness reduction for several classes of CMCs being considered as components in aeroengines [1]. The CMCs are lightweight materials and operate at higher temperature than metals of at least 200°C. In dry air conditions, these materials form a protective layer on the surface called silica which makes them stable at a temperature up to 1300°C for long-term applications. However, in combustion environment containing moisture, the silica layer disintegrates causing surface recession [2]. Therefore, in order for these CMC materials to be useful in aeroengine applications, their surface must be protected. Such protection is being considered by applying environmental barrier coating (EBC) that has a range of operating temperature between 1200 and 1500°C depending on the composition [2–6].

There are three classes of EBC currently being evaluated for SiC/SiC turbine components. They are barium aluminum strontium (BSAS), rare earth di- and monosilicates (REMS and REDS), and hafnia/zirconia based systems [7–9]. The rare earth series include elements from lanthanum to lutetium. In general, an EBC system consists of two or more layers of coating, in which each layer serves a specific purpose. The total thickness of the EBC applied depends on the components and the coating can be applied by different processing methods depending on the intended microstructure and durability. Static components such as combustor liners, turbine vanes, and shrouds are subjected to thermal and gas pressure loads only. As a result, these components can accommodate coating thickness as much as 525 μm. On the other hand, rotating components such

as blades are subjected to a combination of thermal and mechanical loads. To reduce overall weight of the rotating component, the thickness of EBC is limited to ~125 μm [10].

The coating system can be applied via variety of application systems. Among the most common ones are techniques such as air plasma spray (APS), physical vapor deposition (PVD), and slurry depending on the components, manufacturing cost, and intended durability. These systems in general have different material properties than the substrate since the sublayers of the coating are applied at different temperatures and as a result residual stresses develop. Depending on the magnitude and nature of these stresses, damage can occur in the coating after deposition and after exposing the coated substrate to turbine operating conditions. The damage has to be minimized or controlled; otherwise, the coating will spall which will reduce and limit the life of the component [7–9].

Therefore, damage drivers such residual stresses are of concern to EBC development, durability, and application. These stresses can be determined or measured by nondestructive techniques such as X-ray diffraction, Raman spectroscopy, and neutron diffraction. However, because of the complex crystal structure of some of the EBC compositions, it is cumbersome to use these techniques for these measurements. A means to tackling these factors is to control the constituent properties and thickness of the coating and develop physics based models that enable prediction of the durability and service life of the EBC under typical environmental conditions such as moisture, creep, fatigue, and crack propagation at the coating-CMC interface. PFA is used to determine the residual stresses in the specimen and to evaluate their role in damage initiation and propagation.

This paper is an extension of a prior work [1] where the focus of the research was based on examining an analytical methodology to model the durability of the EBC using a multiscale progressive failure analysis [14, 15] approach. Prior work detected damage initiation events using lamina fatigue properties for the CMC as input to the PFA analysis. However, in CMC composites damage initiates at the microscale level of the material. The use of fiber and matrix constituent properties enables the evaluation of damage events at their inception source. With macromechanics, the lamina properties are degraded at the onset of damage. But, with micromechanics, the properties of the constituent that is damaged are degraded, while the other constituent retains its properties.

The analysis used an updated material model for the EBC as compared to the one used in the prior work. Also, it used strength-time exposure degradation model from literature with improved accuracy for the SiC/SiC CMC material. The life prediction was performed once using reverse engineered micromechanics properties as input and once more using macromechanics properties as input. The lamina properties consisted of stiffness, strength, and fatigue properties. Similarly, derived fiber matrix properties consisted of stiffness, strength, and fatigue properties for each constituent. Strength based failure criteria based on maximum stress were employed to determine material damage. Stiffness of damaged elements is reduced once a specific failure criterion is invoked. Damaged elements are not removed from the finite element model. Future work can use fracture mechanics principle using the damage path predicted by PFA to assess fracture growth in the EBC coated CMC specimen. Results from the analytical effort are discussed next.

Table 1: Physical, thermal, and mechanical properties of uncoated SiC/SiC substrate at 21°C [12].

SiC/SiC property	Value	SiC/SiC property	Value
E_{11} (MPa)	$2.85E+05$	S_{11T} (MPa)	$3.21E+02$
E_{22} (MPa)	$2.85E+05$	S_{11C} (MPa)	$3.21E+02$
E_{33} (MPa)	$1.57E+05$	S_{22T} (MPa)	$3.21E+02$
G_{12} (MPa)	$1.13E+05$	S_{22C} (MPa)	$3.21E+02$
G_{23} (MPa)	$9.90E+04$	S_{33T} (MPa)	$4.00E+01$
G_{13} (MPa)	$9.90E+04$	S_{33C} (MPa)	$1.00E+02$
NU12	$1.30E-01$	S_{12S} (MPa)	$2.10E+02$
NU23	$1.70E-01$	S_{23S} (MPa)	$1.05E+02$
NU13	$1.70E-01$	S_{13S} (MPa)	$1.05E+02$
ALPHA11 (1/°C)	$2.71E-06$	ALPHA22 = 33 (1/°C)	$2.71E-06$

2. Description of Analytical Approach

The analyses utilized the finite element method to model the combined EBC/CMC bar specimen sample which included the three layers of EBC and the coated substrate or the CMC part. Finite element model was developed for estimating the stress response based on the known processing conditions of the coating, the specimen geometry of the coated substrate, and the thermomechanical properties of the coated layers and the substrate.

Coating was applied via the plasma spray technique on SiC/SiC composite substrates [9]. It is assumed that the substrate is maintained at 1300°C during deposition of the plasma spray coating and then cooled to room temperature ~25°C. Also, thermomechanical properties of standalone individual layers of the EBC system required for the model were obtained from [13].

The analytical calculations covered modeling the beam specimen with defined EBC layers on top of a SiC/SiC substrate. Thermomechanical properties, including thermal expansion coefficient, stiffness, Poisson's ratio, and strength for all four materials constituting the EBC/CMC specimen, are used as input to the durability and life prediction analysis; see Tables 1 and 2. The SiC/SiC CMC material lamina properties of the fabric were obtained from [12]. Plastic deformation and microcracking that may occur in the plasma-sprayed coating were not considered in the model. The specimen dimensions were 2 by 3 by 45 mm in addition to the EBC thickness on the top, Figure 1. The thermal boundary conditions associated with the coating application methodology were all incorporated into the thermal model.

2.1. Multiscale Progressive Failure Analysis (PFA). Micromechanics and macromechanics composite analysis are integrated with finite element analysis and damage and fracture tracking to perform progressive failure analysis, Figure 2. The capability is integrated in the GENOA [14, 15] software.

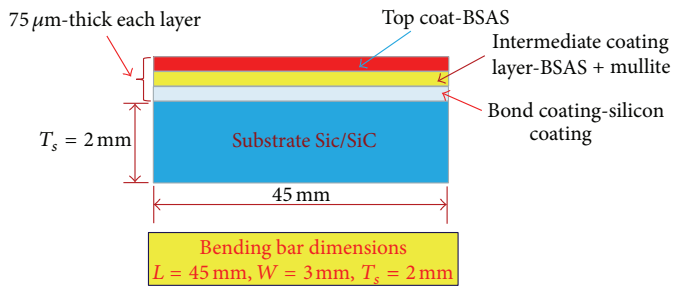

Figure 1: Two-dimensional section of the beam bar specimen showing dimension.

Table 2: Material properties of top and intermediate coats and bond [13].

(a)

Bond coat properties	Value	Units
Young's modulus	97	(GPa)
Poisson's ratio	0.21	(—)
CTE	4.50E − 06	(1/°C)
Tension strength	40	(MPa)
Compression strength	40	(MPa)
Shear strength	40	(MPa)

(b)

Intermediate coat properties	Value	Units
Young's modulus	37.4	(GPa)
Poisson's ratio	0.179	(—)
CTE	5.70E − 06	(1/°C)
Tension strength	28	(MPa)
Compression strength	28	(MPa)
Shear strength	28	(MPa)

(c)

Top coat properties	Value	Units
Young's modulus	32	(GPa)
Poisson's ratio	0.19	(—)
CTE	5.60E − 06	(1/°C)
Tension strength	28	(MPa)
Compression strength	28	(MPa)
Shear strength	28	(MPa)

Traditionally, failure is assessed at the macroscale using lamina or laminate properties. The software enables assessment of failure and damage in composites at a lower scale, that is, the fiber, matrix, and interface level. The methodology augments finite element analysis (FEA), with a full-hierarchical modeling capability that goes down to the microscale of subdivided unit cells composed of fiber bundles and their surrounding matrix [16]. The life prediction strategy uses a PFA-FEA based approach shown in Figure 2 [14, 15].

Damage is tracked at the micro- or macroscale levels leading to local material degradation and recalculation of stiffness. This is done by evaluating series of physics based

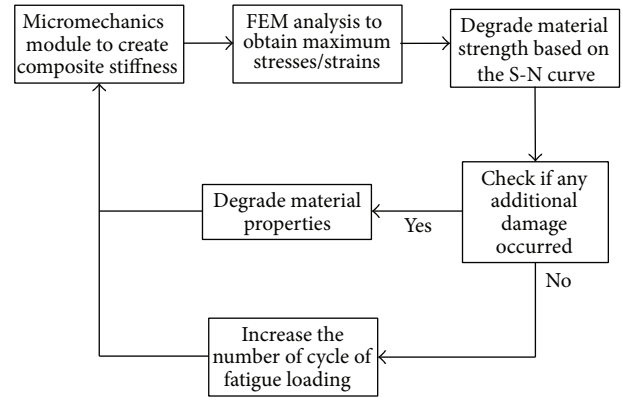

Figure 2: General flow of the progressive failure analysis methodology for life prediction [1].

failure criteria (shown in Table 3) at increased load increments or fatigue cycles. In addition to degradation, stress damage, strength-cycle, or strength-time curves are used as input to the analysis at each fatigue cycle block to degrade the strength. Damage is accumulated as life cycles are increased until the ultimate life of the structure is reached.

The life prediction analysis uses PFA to determine how many cycles of temperature ramping the specimen can sustain before the SiC/SiC and the coating materials are damaged; see Figure 2. Ideally, strength-time curves would be required as input to the analysis for all the materials constituting the EBC/CMC specimen. Such data are typically obtained from physical testing or from literature. The analysis assumed that the EBC coating materials do not degrade as function of exposure time to temperature. Only the SiC/SiC CMC is degraded using test data obtained from literature for strength degradation as function of time [11].

2.2. Life Prediction with PFA. The mathematical approach used in applying the PFA includes the integration of composite mechanics and damage/fracture mechanics with finite element analysis. The damage mechanics account for matrix cracking under transverse, compressive, and shear loading. The ply fracture mechanisms include fiber failure under tension, compression (crushing, microbuckling, and debonding), and delamination. This is invoked via the GENOA code [16] by allowing a sequence of analytical steps that includes

Table 3: Failure criteria used in life prediction of composite specimens.

Mode number	Fiber failure criteria	Event description
1	Longitudinal tensile (S_{11T})	Failure of ply controlled by fiber tensile strength and fiber volume ratio
2	Longitudinal compressive (S_{11C})	(1) Fiber/matrix delamination under compression loading (2) Fiber microbuckling (3) Fiber crushing
3	Transverse tensile	Matrix cracking under tensile loading, event controlled by matrix tensile strength, matrix modulus, and fiber volume ratio
	Transverse compressive	Matrix cracking under compressive loading, event controlled by matrix compressive strength, matrix modulus, and fiber volume ratio
	Normal tensile (S_{22T})	Plies are separating due to normal tension
4	Normal compressive (S_{22C})	Due to very high surface pressure that is crushing of laminate
5	In-plane shear (S_{33C})	Failure in-plane shear relative to laminate
6	Transverse normal shear (S_{12S})	Shear failure acting on transverse cross-oriented in a normal direction of the ply
7	Longitudinal normal shear (S_{13S})	Shear failure on longitudinal cross section that is oriented in a normal direction of ply
	Normal tensile (S_{23T})	Combined stress failure criteria used for isotropic materials
	Relative rotation criterion (RROT)	Considers failure if the adjacent plies rotate excessively with one another
8	Transverse normal shear (S_{23S})	Considers invariant through-the-thickness
9	Linear elastic fracture	Virtual crack closure technique (VCCT), discrete cohesive zone model (DCZM)

(1) the use of a finite element stress solver, (2) user selection of 2D or 3D architectural details (through-the-thickness fibers, resin rich interphase layer between weave plies, fiber volume ratio, void shape, size and location, cure condition, etc.), (3) assigning static (thermomechanical) or spectrum loading, (4) automatic update of the finite element model prior to executing FEA stress solver for accurate lamina and laminate properties, and (5) degradation of material properties at increased loading (including number of cycles) based on detected damage. Additional details can be found in [14].

All stages of damage evolution within the composite structure are identified. They are damage initiation, damage propagation, fracture initiation, and fracture propagation. The damage events include matrix cracking, delamination, and fiber failure. Displacements, stresses, and strains derived from the structural scale FEA solution at a node or element of the finite element model are passed to the laminate and lamina scales using laminate theory. Stresses and strains at the microscale are derived from the lamina scale using microstress theory. The analytical capability offers microscale modeling and damage assessment capability for composite materials such as ceramic, metal, and polymer matrix composites. For the failure criteria shown in Table 3, the code automatically distinguishes between the criteria that are applicable to laminated composites versus those that are applicable to isotropic material. For example, for longitudinal compression, the code evaluates three failure potentials under longitudinal compression. They are fiber and matrix delamination, fiber microbuckling, and fiber crushing. For isotropic materials, the compression stress or strain is compared to the allowable to determine whether or not failure had occurred. In addition to maximum stress failure criteria, the code evaluates failure due to maximum strain and interactive stress criteria. More details can be obtained from [14, 15].

PFA stress based evaluation is accurate up to fracture initiation [14, 15]. Due to stress singularity often experienced in finite element analysis, fracture mechanics based approach is used to grow the crack. In linear fracture mechanics approach, it is required to have fracture toughness for static crack growth and da/dn versus ΔK for fatigue crack growth; da/dn is the change of crack length with loading cycles, while ΔK is the stress intensity factor change. Since such data are not available for the analysis, the focus in this paper is to identify cycles that caused damage to initiate and propagate to the substrate SiC/SiC material. It should be noted that the PFA strength based approach has key advantages as compared to fracture mechanics methods. For example, in terms of advantages, PFA does not require prior knowledge of crack path. Crack growth will be the subject of future work once the data required for the prediction becomes available.

Additionally, for the analyses used in this paper, linear elastic fracture mechanics approach (item no. 9 in Table 3) is not used. Fracture mechanics application would require knowledge of fracture path, toughness, and fracture energy. This type of analysis will be considered in the future.

3. Specimen Geometry and FE Model

The finite element analyses to generate the thermal profile were conducted using the commercial finite element code

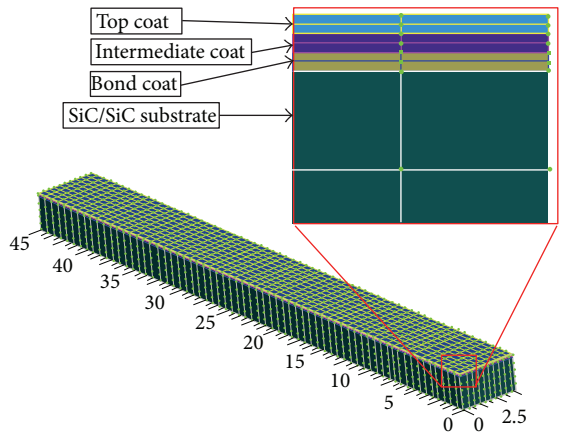

Figure 3: Representative finite element model of the thermal barrier coating. Work plane rulers shown are in units of mm.

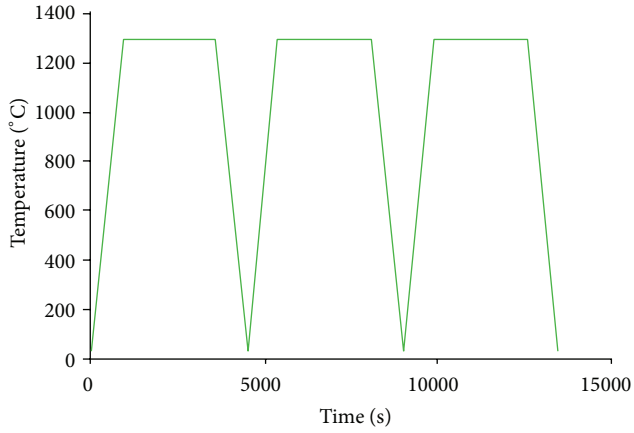

Figure 4: Representative thermal loading profile applied in the analyses.

Abaqus [17]. The finite element model dimensions and sections are shown in Figure 3. The thermal profile was predicted under transient loading conditions as noted in Figure 4. The thermal cycle assumes that the bar specimen is initially at 21°C and, within 15 minutes, it heats up to 1300°C and remains constant for a duration of 45 minutes until shutdown, where it cools off back to 21°C. One complete cycle constitutes exposing the specimen to these thermal conditions for a total time of one hour. Material properties of both the coating and the substrate were input into the model under linear isotropic condition for the coating systems and linear orthotropic condition for the SiC/SiC substrate. Temperature dependency of all the materials was accounted for in the analyses. The mesh included a 3D model of the bar specimen with high density mesh along the substrate and the coatings interfaces. Eight-node brick element was employed.

For the durability solution, GENOA-PFA augmented the FEA solver (Abaqus) for life prediction to determine life cycles that caused damage to initiate and propagate. PFA used Abaqus iteratively at increased number of cycles to evaluate damage after each FEA run. Damage stabilization is attained to ensure material and structural equilibrium before the number of cycles is increased again. The process is repeated until ultimate life is obtained. It was assumed that the top coat BSAS, intermediate coating layer (BSAS+Mullite), and the bond silicon coating do not degrade as a function of time and temperature and the results presented pertained only to determining the number of cycles that it would take for damage to initiate and for damage to propagate. Furthermore, data obtained from literature [11] shows that some degradation of the SiC/SiC substrate at elevated temperature after exposure time is expected.

4. Analytical Description

To evaluate the effects of thermal fatigue on the EBC SiC/SiC using micromechanics based approach, in situ (effective) fiber and matrix properties for the SiC/SiC system were generated. To generate the effective SiC/SiC constituent properties, a [0, 90]s laminate with 50% fiber volume content was modeled using materials characterization and qualifications (MCQ) composite software [18] and an iterative process (Figure 5) was implemented. The code used an optimization algorithm to derive a unique set of fiber/matrix properties (mainly stiffness and strength) that are capable of reproducing test data of the lamina or laminate. The process iterates until values of the predicted lamina or laminate in-plane and out-of-plane properties are in good agreement with data from test. The fiber and matrix properties for the SiC/SiC derived through the elaborate reverse engineering process shown in Tables 4(a) and 4(b) are used as input to PFA to determine the life cycle that would cause damage to initiate and propagate in the CMC specimen. This makes it possible to run the comparative assessment of the behavior of the CMC using both microscale (fiber and matrix) and macroscale (lamina level). PFA treats the top, intermediate, and bond materials as isotropic during the life prediction analysis.

The fiber and matrix properties obtained from reverse engineering are listed in Table 4(a). The fiber and matrix properties are then used as input to MCQ [18] to evaluate the mechanical properties of the CMC (0/90)s laminate. As indicated in Table 4(b), the MCQ predictions starting from microscale properties yielded an accurate representation of the laminate properties from test [12]. The out-of-plane predictions for the laminate could improve as the properties were taken from a plain weave system where the effects of the fiber weave on the out-of-plane strength and stiffness was significant. If more details were available on the architecture, the out-of-plane predictions with MCQ would improve as the architecture details would be included in material characterization.

4.1. SiC/SiC Stress-Cycle Curve as Function of Exposure Time. The stress cycle (S-N) criterion adopted for these analyses utilized a set of S-N curve for each of the laminate, fiber, and matrix as shown in Figure 6. The first set used the typical or the standard S-N curve that represented the degradation of the SiC/SiC composite under thermal loading conditions [11]. This S-N curve started to degrade after 27.78 hours

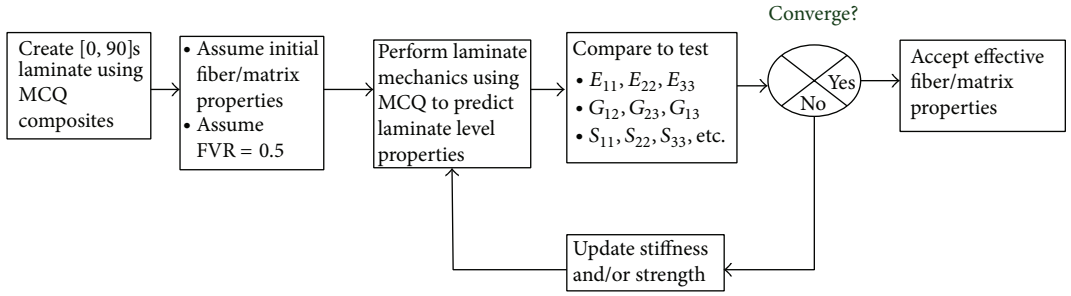

Figure 5: Iterative process used to determine effective constituent properties of SiC/SiC laminate.

Table 4: (a) Effective fiber and matrix properties. (b) Effective ply correlating to effective fiber/matrix properties.

(a)

Effective fiber and matrix properties (FVR = 0.5 [0, 90]s)					
SiC fiber			SiC matrix		
Property	Units	Value	Property	Units	Value
E_{11}	MPa	380000	E	MPa	380000
E_{22}	MPa	156000	NU		0.19
G_{12}	MPa	100000	ST	MPa	250
G_{23}	MPa	70000	SC	MPa	250
NU12		0.19	SS	MPa	190
NU23		0.17	ALPHA	1/degC	$2.71E-06$
S_{11T}	MPa	600			
S_{11C}	MPa	600			
ALPHA11	1/degC	$2.71E-06$			
ALPHA22	1/degC	$2.71E-06$			

(b)

Properties of [0, 90]s using effective fiber/matrix properties				
Property	Units	Target values	Calibrated	Discrepancy (%)
E_{11}	MPa	284900	285000	0.0
E_{22}	MPa	284900	285000	0.0
E_{33}	MPa	190600	157000	17.6
G_{12}	MPa	112300	113000	0.6
G_{23}	MPa	104800	99000	5.5
G_{13}	MPa	104800	99000	5.5
NU12	MPa	0.126	0.13	3.2
NU23	MPa	0.2132	0.17	20.3
NU13	MPa	0.2132	0.17	20.3
S_{11T}	MPa	318.5	321	0.8
S_{11C}	MPa	318.5	321	0.8
S_{22T}	MPa	318.5	321	0.8
S_{22C}	MPa	318.5	321	0.8
S_{12S}	MPa	213.5	210	1.6

from 318 MPa to 159 MPa (50% of the original ultimate tensile strength at $t = 0$) at 1000 hr. The logarithmic degradation continued until failure. Since S-N curve was not available for the constituent materials, it was assumed that the same degradation trends occurred for the fiber and matrix

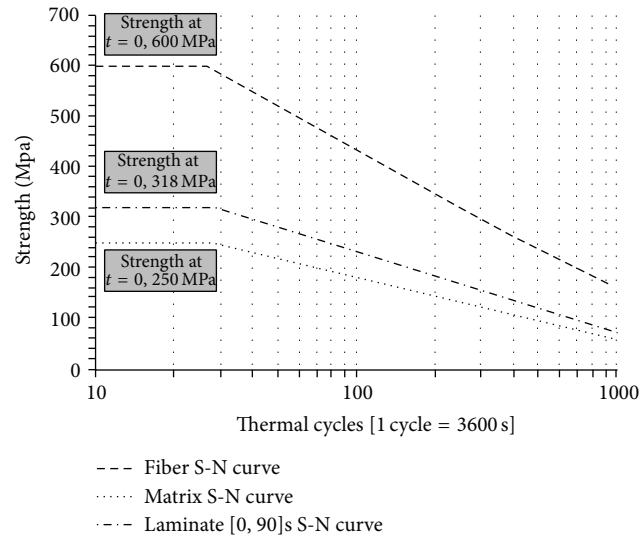

Figure 6: Strength as a function of thermal cycles for laminate, fiber, and matrix of SiC-SiC material [11].

level. To achieve these trends, the laminate level trend was scaled accordingly using the fiber and matrix ultimate tensile strength at $t = 0$.

Characteristics and thickness dimensions of the coating system used are shown in Table 5 and, as noted, the 3 layers of coating had the same magnitude of thickness which is 75 μm and the substrate had a 2 mm thickness. Photographs of the top surface and cross section of a typical APS trilayered environmental barrier coated SiC/SiC composite are shown in Figure 7. The sublayers of the coating are inhomogeneous and contain microcracks and significant levels of nonuniform pores.

5. Results and Discussion

The durability analysis performed indicated that the material damage initiated in the top EBC coat and then propagated down to the intermediate layer then to the bond. This took place during the first one hour of thermal loading (in one cycle). For each cycle, the PFA analysis assumed that the specimen reached the 1300°C temperature, which means that a gradient of 1279°C is applied instantly to simulate each cycle.

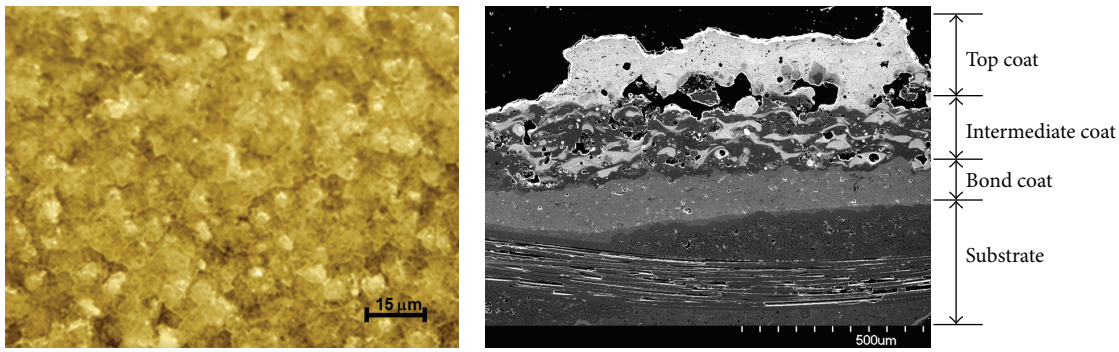

(a) (b)

Figure 7: Typical microstructure of plasma sprayed EBC on SiC/SiC composites: (a) top view (optical micrograph) and (b) cross-sectional view (scanning electron micrograph).

Table 5: Coating systems and thicknesses considered.

Coating system	Coating thickness
Top coat-BSAS	75 μm
Intermediate coat Mullite + barium strontium aluminum silicate (BSAS)	75 μm
Bond coat-silicon	75 μm
Sic-SiC substrate	2 mm

Table 6: Summary of cycles to damage and associated damage modes for each EBC and substrate layer.

Layer	Cycle of damage initiation	Damage mode
Top layer	1	Tension
Intermediate layer	1	Tension and shear
Bond layer	1	Tension and shear
SiC/SiC	Macro: 1070 Micro: 1090	Tension

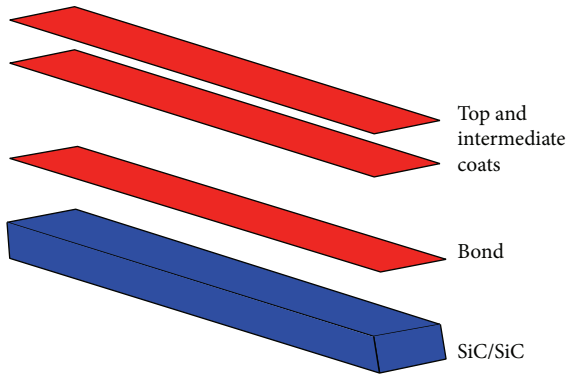

Figure 8: Damage in the EBC layers due to tension stress (red color indicates damage; blue color represents undamaged elements).

As mentioned earlier in the paper, the maximum stress criteria listed in Table 3 are used in the durability evaluation performed by the PFA. When an element stress exceeds the allowable value, the stiffness of the element was degraded accordingly in the direction where the damage occurred. No elements were removed when damaged, which meant that the mesh size remained unchanged throughout the analysis. The analysis was repeated twice, once with macrolevel properties for the CMC material and once more with microlevel properties using the reverse engineered properties of the fiber and matrix.

Figure 8 shows the damaged elements in red color in the three EBC layers due to tension stress. As noted, all elements in the three EBC layers are damaged at the end of cycle 1, that is, after 3600 seconds of exposure to 1300°C. The damage started in the top layer and propagated down to the bond. The SiC/SiC substrate was undamaged until the cycle 1070 was reached for macrotype input and until the cycle 1090 for micro input.

The damage volume is computed to keep track of total number of elements that are damaged during a given loading cycle. It provides useful inspection criterion of critical parts. For example, a sudden increase in damage volume indicates the onset of major damage event in the structure. Since only degradation in the SiC/SiC substrate was considered, no additional damage was detected until cycle 1070 when the SiC/SiC substrate's tensile failure criterion was detected. A summary of the life cycles for the EBC-SiC/SiC system is shown in Table 6. A macrobased simulation seemed to offer more conservative life cycle compared with the microbased approach showing greater life by approximately 20 hours. This is assuming the same in-plane ply properties and when using effective fiber/matrix properties rather than macrobased laminate properties.

The results indicated that macromechanics or ply mechanics approach is more conservative when it comes to assessing damage initiation in the substrate as compared to microscale simulation. This was expected as the postdamage degradation was more severe at the macrolevel as compared to the one at the microscale. With micromechanics, if one

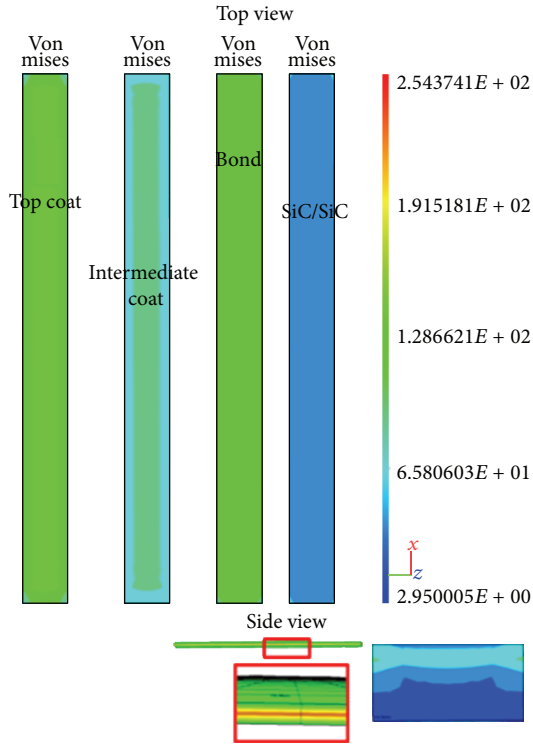

Figure 9: Von Mises residual stresses in MPa as a result of cool down from 1300°C to room temperature after the first cycle of exposure to elevated temperature (top and side views).

constituent is damaged, the other constituent retains the stiffness. In the case of macromechanics approach, the whole lamina stiffness in the direction of damage is reduced to a small value.

Figure 9 shows the von Mises residual stresses in each material obtained during cool down from 1300°C to room temperature. The residual stresses are a good indicator of where damage is likely to start. It supports the findings presented in Figure 9, whereby the top, intermediate, and bond layers were damaged first before propagating after several hundred cycles to the CMC substrate. The PFA analysis is accounting for the residuals' stresses during the life prediction as the residual stresses are translated into damage indices when damage is introduced. The damage indices are then stored for use as input in the subsequent cycle analysis.

It should be further noted that the von Mises stresses calculated during cool down show that the bond material experienced the highest stresses. However, this does not mean that the bond is failing more than the top or intermediate coats. Failure is driven by the allowable material stress or strain. In the case of the EBC specimen, the maximum stress criteria were used to guide the assessment of the damage evolution. Comparing stress to strength for the top three materials, the residual stresses do indicate that material damage is experienced by all three materials, whereby the top coat experienced the most damage because of the ratio of stress to strength. Future analysis will include material nonlinearity as well as coupled structural thermal analysis to determine the effect of nonuniform heating on the specimen's life prediction.

6. Conclusions and Future Work

A novel computational simulation approach is presented to predict life for EBC/CMC specimen using the finite element method augmented with progressive failure analysis (PFA) that included durability, damage tracking, and material degradation model. The following conclusions and recommendations can be drawn from the work presented in the paper.

(1) Damage initiates predominately in the top coat due to tensile strength failure and in the intermediate/bond coat due to delamination.

(2) Damage propagates into the SiC/SiC substrate due to tensile failure, eventually redistributing the stress into the EBC causing further damage propagation.

(3) Multiscale progressive failure analysis allowed a systematic prediction of the life cycles for damage initiation and propagation in EBC SiC/SiC specimens. The technical approach applied combined composite mechanics and damage tracking and fracture.

(4) Use of micromechanics properties as input to PFA resulted in life prediction that is approximately 20 hours greater as compared to that obtained from the

use of lamina properties indicating that macromechanics is more conservative than micromechanics.

(5) Accurate life prediction requires strength-time exposure behavior for all the materials used in the specimen. This will allow reliable assessment of any structural component made of the same materials.

(6) Defects such as flaws and initial cracks in coating will add more accuracy to the life prediction analysis and it all must be accounted for in any future work.

(7) Material characterization can help optimization of the laminate thickness which in return can increase life and delay damage.

(8) Material architecture should be considered in the material characterization to yield an accurate reverse engineering of constituent properties.

(9) Future work should include nonlinear material behavior in the analysis and simulations performed. This will require data from ATSM tests at different temperatures.

Nomenclature

E_{11}: Lamina modulus in fiber direction
E_{22}: Lamina modulus perpendicular to fiber direction
E_{33}: Lamina modulus perpendicular to fiber direction
G_{12}: Lamina in-plane shear modulus
S_{11C}: Lamina compressive strength in fiber direction
S_{11T}: Lamina tensile strength in fiber direction
S_{12S}: Lamina in-plane shear strength
S_{22C}: Lamina compressive strength perpendicular to fiber direction
S_{22T}: Lamina tensile strength perpendicular to fiber direction
S_{13}: Lamina strength in longitudinal shear direction
S_{23}: Lamina strength in transverse shear direction
S_{33T}: Lamina tensile strength in normal out-of-plane direction
S_{33C}: Lamina compressive strength in normal out-of-plane direction
Alpha11: Thermal expansion coefficient in fiber direction
Alpha22: Thermal expansion coefficient transverse to fiber direction
Alpha33: Thermal expansion coefficient normal to fiber direction
da/dn: Change of crack length with loading cycles
ΔK: Stress intensity factor change.

Conflict of Interests

The authors declare that there is no conflict of interests regarding the publication of this paper.

References

[1] A. Abdul-Aziz, G. Abumeri, W. Troha, R. T. Bhatt, J. E. Grady, and D. Zhu, "Environmental barrier coating (EBC) durability modeling using a progressive failure analysis approach," in *Smart Structures and Materials & Nondestructive Evaluation and Health Monitoring, Behavior and Mechanics of Multifunctional and Composite Materials*, vol. 8346 of *Proceedings of SPIE*, San Diego, Calif, USA, March 2012.

[2] K. N. Lee, D. S. Fox, R. C. Robinson, and N. P. Bansal, "Environmental barrier coatings for silicon-based ceramics," in *High Temperature Ceramic Matrix Composites*, W. Krenkel, R. Naslain, and H. Schneider, Eds., pp. 224–229, Wiley-Vch, Weinheim, Germany, 2001.

[3] P. J. Jorgensen, M. E. Wadsworth, and I. B. Cutler, "Oxidation of silicon carbide," *Journal of the American Ceramic Society*, vol. 42, no. 12, pp. 613–616, 1959.

[4] J. L. Smialek, R. C. Robinson, E. J. Opila, D. S. Fox, and N. S. Jacobson, "SiC and Si_3N_4 recession due to SiO_2 scale volatility under combustor conditions," *Advanced Composite Materials*, vol. 8, no. 1, pp. 33–45, 1999.

[5] K. L. More, P. F. Tortorelli, and L. R. Walker, "Effects of high water vapor pressures on the oxidation of SiC-based fiber-reinforced composites," *Materials Science Forum*, vol. 369—372, pp. 385–394, 2001.

[6] K. L. More, P. F. Tortorelli, L. R. Walker, N. Miriyala, J. R. Price, and M. Van Roode, "High-temperature stability of SiC-based composites in high-water-vapor-pressure environments," *Journal of the American Ceramic Society*, vol. 86, no. 8, pp. 1272–1281, 2003.

[7] K. N. Lee, "Current status of environmental barrier coatings for Si-based ceramics," *Surface and Coatings Technology*, vol. 133-134, pp. 1–7, 2000.

[8] D. M. Zhu, R. A. Miller, and D. S. Fox, "Thermal and environmental barrier coating development for advanced propulsion engine systems," NASA TM-2008-215040, 2008.

[9] D. M. Zhu, N. P. Bansal, and R. A. Miller, "Thermal conductivity and stability of HfO_2-Y_2O_3 and $La_2Zr_2O_7$ evaluated for 1650°C," in *Advances in Ceramic Matrix Composites*, N. P. Bansal, J. P. Singh, W. M. Kriven, and H. Schnneider, Eds., John Wiley & Sons, Hoboken, NJ, USA.

[10] D. Zhu and R. A. Miller, "Thermal conductivity and elastic modulus evolution of thermal barrier coatings under high heat flux conditions," *Journal of Thermal Spray Technology*, vol. 9, no. 2, pp. 175–180, 2000.

[11] S. Ochiai, S. Kimura, H. Tanaka et al., "Degradation of SiC/SiC composite due to exposure at high temperatures in vacuum in comparison with that in air," *Composites A: Applied Science and Manufacturing*, vol. 35, no. 1, pp. 33–40, 2004.

[12] M. van Roode, A. K. Bhattacharya, M. K. Ferber, and F. Abdi, "Creep resistance and water vapor degradation of sic/sic ceramic matrix composite gas turbine hot section components," in *ASME Turbo Expo 2010: Power for Land, Sea, and Air*, pp. 455–469, June 2010.

[13] A. Abdul-Aziz and R. T. Bhatt, "Modeling of thermal residual stress in environmental barrier coated fiber reinforced ceramic matrix composites," *Journal of Composite Materials*, 2011.

[14] M. Garg, G. H. Abumeri, and D. Huang, "Predicting failure design envelop for composite material system using finite element and progressive failure analysis approach," in *Proceedings of the 52nd International SAMPE Symposium: Material and Process Innovations: Changing our World (SAMPE '08)*, May 2008.

[15] F. Abdi, Z. Qian, and M. Lee, *The Premature Failure of 3D Woven Composites*, ACMA Composites, Columbus, Ohio, USA, 2005.

[16] "GENOA durability and damage tolerance and life prediction software," AlphaSTAR Corporation, Long Beach, Calif, USA, http://www.ascgenoa.com.

[17] "Abaqus commercial finite element code," Providence, RI, USA, 2909—2499.

[18] "MCQ software," AlphaSTAR Corp, Long Beach, Calif, USA, 2012.